ACS ES&T Air

Open Access

pubs.acs.org/estair

Article

Analyzing the Role of Chemical Mechanism Choice in Wintertime $PM_{2.5}$ Modeling for Temperature Inversion-Prone Areas

Published as part of ACS ES&T Air special issue "John H. Seinfeld Festschrift".

Cam M. Phelan,* Abiola S. Lawal, Jacob Boomsma, Kamaljeet Kaur, Kerry E. Kelly, Heather A. Holmes, and Cesunica E. Ivey

Cite This: ACS EST Air 2025, 2, 162−174

Read Online

ACCESS | Metrics & More | Article Recommendations | Supporting Information

ABSTRACT: Chemical transport models are used for federal compliance demonstrations when areas are out of attainment, but there is no guidance for choosing a chemical mechanism. With the 2024 change of the annual $PM_{2.5}$ standard and the prevalence of multiday wintertime inversion episodes in the western U.S., understanding the wintertime performance of chemical transport models is important. This study explores the impact of chemical mechanism choice on the Community Multiscale Air Quality (CMAQ) model performance for $PM_{2.5}$ and implications for attainment demonstration in inversion-prone areas in the western United States. Total and speciated $PM_{2.5}$ observations were used to evaluate wintertime CMAQ simulations using four chemical mechanisms. The study evaluated intermechanism differences in total and secondary $PM_{2.5}$ and the impact of meteorology at sites with observed multiday temperature inversions. Model performance for total $PM_{2.5}$ was similar across chemical mechanisms, but intermechanism differences for total and secondary $PM_{2.5}$ were exacerbated during inversion periods, suggesting that modeled chemistry contributes to the model bias. Results suggest that nitrate, ammonium, and organic carbon are secondary species for which model results do not agree or perform to standard evaluation metrics in scientific literature. These findings show a need for mechanistic investigations of the causes of these differences.

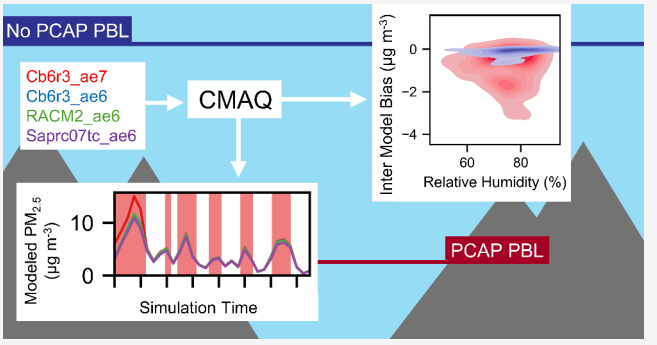

KEYWORDS: *air quality, secondary aerosols, CMAQ, PCAP, environmental modeling, CSN*

1. INTRODUCTION

The majority of the fine particulate matter ($PM_{2.5}$) National Ambient Air Quality Standards (NAAQS) nonattainment areas are in the western U.S., and is projected to remain so.[1] Poor air quality in this region can be exacerbated by topographical features that inhibit outflow during extreme meteorological conditions. One such condition, a persistent cold air pool event (PCAP), occurs when cold air is trapped for multiple days in a valley or basin resulting in a stable layer of air (colloquially referred to as a temperature inversion).[2,3] These events occur often during wintertime in the Intermountain West and could occur more frequently as a result of predicted increases in high pressure subsidence, though warmer winters and decreased snow cover from a changing climate could have the opposite effect.[4−8] PCAPs often lead to elevated pollutant concentrations, which is concerning, given that exposure to fine particulate matter is a known risk factor for both chronic and acute adverse health impacts and that these exposures are often elevated during PCAPs.[9−16]

The U.S. EPA lowered the primary NAAQS for $PM_{2.5}$ to an annual mean of 9 $\mu g\ m^{-3}$ in February of 2024, a 25% decrease from the previous standard set in 2012.[17] When an administrative region or county is out of attainment, the Community Multiscale Air Quality (CMAQ) model or a similar chemical transport model is often used to demonstrate that proposed emission controls will bring nonattainment areas into attainment in the future.[18−20] These models tend to cover the full year for the annual $PM_{2.5}$ NAAQS and several days surrounding a period of elevated $PM_{2.5}$ for the 24-h NAAQS.[21] EPA provides detailed guidance and instructions for running demonstration models of ozone and $PM_{2.5}$, but does not provide specific guidance on choosing a gas-phase chemical mechanism, aerosol module, or meteorological model configuration options.[19,21] This is intended to give flexibility to attainment modelers, and does require a demonstration that

Received: June 14, 2024
Revised: January 1, 2025
Accepted: January 2, 2025
Published: January 10, 2025

the mechanism selected performs reasonably versus observations.[19] CMAQ simulations are computationally expensive, however, and mechanisms that perform to expectations in one season may not perform as well in another.

Previous studies have shown that meteorological parameters are significantly different during PCAP episodes, including the PCAP formation and dissipation periods.[2,3,22] This includes elevated relative humidity, lower planetary boundary layer heights, reduced wind speeds, and colder temperatures.[2,15,22−26] There is also a well-documented issue with correctly capturing boundary layer dynamics during PCAPs in meteorological models.[3,22,23,27] This can have significant impacts on simulated aerosol and gas-phase concentrations, and any uncertainty within the meteorological inputs is also propagated through the chemical transport model.[28]

The carbon bond (CB) mechanisms use explicit organic species and lumped-structure groups that represent the remaining organic species. This lumped-structure method is essentially a sum of basic carbon bond types. While the first CB mechanism was created in the 1970s, the versions used here were specifically developed to better represent wintertime ozone events in the Rocky Mountains by modifying the rate equations to reduce the formation rate of alkyl nitrates at low temperatures.[29,30] CMAQ features two versions of the cb mechanism that are commonly used in recent studies, *cb6r3_ae6_aq* and *cb6r3_ae7_aq*.[31] Mechanism *cb6r3_ae6_aq* tracks 60 explicit and 68 lumped species, and *cb6r3_ae7_aq* tracks 62 explicit and 66 lumped species.[32] The significant differences between AERO7 and AERO6 are an extra pathway for the formation of glyoxal and updated monoterpene chemistry in AERO7.[20,33,34]

The RACM2 (*racm2_ae6_aq* in CMAQ) mechanism used is built upon the Regional Acid Deposition Model (RADM), which was developed to study the formation of atmospheric acids, organic and inorganic peroxides, and aqueous oxidation of SO_2 in the atmosphere.[30,35] RACM2 expands upon this by explicitly including organic compounds that are significant reactants in a low-NOx atmosphere.[30,35] Mechanism *racm2_ae6_aq* tracks 54 explicit and 80 lumped species and uses AERO6 chemistry for aerosols.[32]

The SAPRC07 mechanism (*saprc07tc_ae6_aq* in CMAQ) is built upon the SAPRC99 mechanism, which was originally developed in 1999 to study ozone formation and VOCs.[30,36] SAPRC07 improved upon SAPRC99 by updating reaction and photolysis rates, adding chlorine chemistry with aldehydes and ketones, and updated treatment of peroxy radicals[36−38] This was done with the goal of better representing secondary organic aerosol and hydroperoxide formation. Mechanism *saprc07tc_ae6_aq* tracks 97 explicit and 64 lumped species, but more detailed versions can track up to 780 explicit organics (to the detriment of computational efficiency).[30,32] This mechanism also uses AERO6 aerosol chemistry.

These differences between gas-phase and aerosol-phase mechanisms have been shown to influence simulated concentrations of air pollutants, especially biogenic VOCs and nitrogen species important for nighttime chemistry.[30,39,40] The question we aim to address in this work is how these differences change with meteorology in the Intermountain West, especially meteorology associated with PCAPs. In this study, we compare the results of four CMAQ simulations for five sites in the western U.S. that are prone to elevated $PM_{2.5}$ concentrations and wintertime PCAPs. We investigate the impact of gas-phase chemical mechanism and aerosol module choices on 24-h NAAQS attainment for $PM_{2.5}$. Using model meteorology and observed PCAP episodes, we also explore intermechanism differences for secondary $PM_{2.5}$ during these events. We then examine the relative performance of each mechanism for chemically speciated $PM_{2.5}$ at the study sites with speciated $PM_{2.5}$ measurements from the Chemical Speciation Network (CSN).

2. MATERIALS AND METHODS

2.1. Chemical Transport Modeling. Four CMAQ 5.3.3 simulations were conducted over January 2016 plus 2 weeks spin-up time, using a 12 km horizontal domain over continental U.S. and 35 vertical layers, 14 of which were within 1 km above the surface.[32,41,42] Model A used the default model chemistry (cb6r3 gas-phase chemistry with AERO7 aerosol module).[43,44] Model B used the cb6r3 chemistry but used the AERO6 module instead of AERO7. Model C used the RACM2 gas-phase chemistry with AERO6.[35] Model D used SAPRC07tc gas-phase chemistry with AERO6.[36,38]

All simulations used the 2016 base year emissions from the National Emissions Inventory Collaborative 2016beta platform provided by the EPA[45] and meteorology from an offline Weather Research and Forecasting (WRF) version 4.3.3 simulation. The WRF simulation used one of the parametrization options tested in Sun et al. (2021)[23] with the same vertical levels. The planetary boundary layer (PBL), surface layer, and land surface model options were selected to be consistent with the PBL physics and vertical diffusion in CMAQ.[46,47] The 12 km horizontal grid used here is not representative of typical SIP models or the Sun paper, which use 4 km grids. This coarser grid is also insufficient for resolving the meteorology common during PCAPs, as discussed below in Section 3.3. Even 4 km grids are not capable of resolving this meteorology in the Salt Lake Valley, however.[16,48] With these caveats, we do not expect to see good performance from any simulations in this application but are still able to compare how the mechanisms behave with varying meteorological conditions in the western U.S. wintertime, which is the goal of the study. See Table 1, below, for more details on the WRF and CMAQ model configurations.

All CMAQ outputs were processed to analyze the following data at an hourly frequency: total, primary, secondary, and chemically speciated $PM_{2.5}$ concentrations. Total and chemically speciated $PM_{2.5}$ concentrations were generated with the CMAQ postprocessing combine tool using mechanism-specific species definition files provided in the tool source code. As CMAQ does not explicitly track primary and secondary PM, we defined these species independently. We defined secondary aerosol species as the following model variables in CMAQ: ASOMIJ (secondary organic matter), ASO4JK (aerosol sulfate), ANO3IJK (aerosol nitrate), ANH4IJK (aerosol ammonium), and ACLIJK (aerosol chloride). This is converted to $PM_{2.5}$ concentrations in the CMAQ combine script, which multiplies the above aerosol species at all available modes by modeled aerosol size distributions (from APMDIAG files) to get CSN-equivalent concentrations of $PM_{2.5}$.[32] This was based on previous studies, the structure of the CMAQ aerosol module, and advice from the CMAS User Forum.[59−64] We then defined primary $PM_{2.5}$ as the difference between the modeled total $PM_{2.5}$ (PM25_TOT in the model) and the calculated secondary $PM_{2.5}$.

Modeled surface relative humidity, temperature, horizontal wind speed at 10 m above ground level, and PBL height were

https://doi.org/10.1021/acsestair.4c00139
ACS EST Air 2025, 2, 162−174

Table 1. CMAQ v5.3.3 and WRF v4.3.3 Specifications

Model Option	Configuration
Chemical mechanisms	A: cb6r3_ae7_aq; B: cb6r3_ae6_aq; C: racm2_ae6_aq; D: saprc07tc_ae6_aq;
Spatial grid	12 km by 12 km horizontal grid; 35 vertical levels (14 under 1 km above the surface)
Biogenic emissions processing	BEIS3 inline emissions
Potential combustion secondary organic aerosols (pcSOA)	Model default: emissions of POC and PNCOM from nonfire sources scaled by a factor of 6.579 and applied as PCVOC emissions[49]
Inline wind-blown dust emissions	Turned on (model default)
Bidirectional ammonia flux	Turned on (model default)
Ocean halogen chemistry	Turned on (model default)
Deposition scheme	M3dry (model default)
Meteorological processor	MCIP5.3.3
Planetary boundary layer scheme	Asymmetric Convective Model 2 (ACM2)[50]
Land surface model	Pleim-Xiu[46,51]
Surface layer	Pleim[52]
Microphysics	Thompson[53,54]
Radiation	Dudhia shortwave[55] and RRTM longwave[56,57]
Cumulus parametrization	Kain-Fritsch[58]

the meteorological variables of interest. These are consistent across the CMAQ simulations, as the WRF simulation used for meteorology was run offline and not coupled with CMAQ. WRF-generated PBL height estimates are used for comparing CMAQ simulation results, but modeled meteorology was compared with soundings using the bulk Richardson number approach.[65−67] These meteorological variables were extracted from WRF and compared with observational data in the same grid cell to evaluate the meteorological inputs.

2.2. Monitoring Site Descriptions and Observational Data. We chose five sites for analysis corresponding to four U.S. locations previously examined for PCAP dynamics (Colgan et al. 2021),[3] where two of the sites are in neighboring areas in northern Utah stations (Figure 1). Observational data for total $PM_{2.5}$ (parameter codes 88101 and 88502) were accessed through the EPA AQS API on the sample level and then averaged by day. See Table 2, below, for site locations, station names accessed for observational data, and other information.

PCAPs were determined using twice daily radiosonde observations in Reno, Denver, Salt Lake City, and Boise. These data were obtained from the University of Wyoming Upperair Air Data repository.[68] Vertical profiles of temperature, humidity, and windspeed were visualized on thermodynamic plots (skew T-log P diagrams) to visually determine the presence of a CAP and were characterized qualitatively using yes/no/maybe. CAP cases ("yes") had vertical profiles with either a temperature inversion, isothermal layer, or a profile indicative of a stable atmospheric boundary layer. Cases labeled "no" had no stable layer or had a surface wind speed greater than 10 m s^{-1} if there was a weak stable layer. The

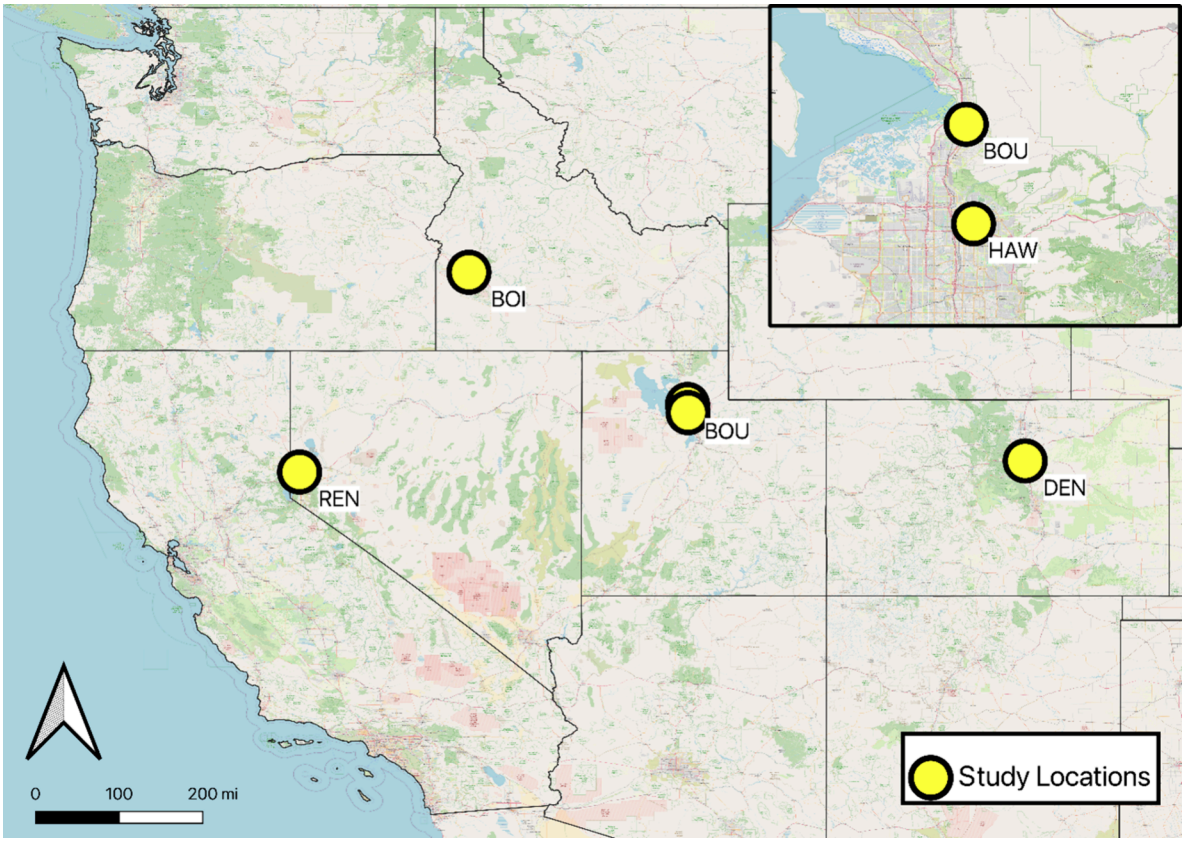

Figure 1. Map of the radiosonde study sites in the western United States in areas prone to multiday inversions.[3] Inset shows the relative locations of the two Utah sites: Bountiful and Hawthorne. All sites are also Chemical Speciation Network (CSN) stations, reporting chemically speciated $PM_{2.5}$ concentrations every third or sixth day.

https://doi.org/10.1021/acsestair.4c00139
ACS EST Air 2025, 2, 162−174

Table 2. Study Site Locations and Observational and Topographic Information[a]

Site Name	AQS Site ID	Coordinates (WGS84)	Floor Height (m)	Ridge Height (m)	Balloon Site	Surface Met. Site	# PCAP Days
Boise	16−001−0010	43.600699, −116.347853	830	1829	BOI	KBOI	17
Bountiful	49−011−0004	40.902967, −111.884467	1289	2438	SLC	KSLC	23
Hawthorne	49−035−3006	40.736389, −111.872222	1289	2438	SLC	KSLC	23
Denver	08−031−0002	39.751184, −104.987625	1611	2743	DNR	KDNR	15
Reno	32−031−0016	39.525083, −119.807717	1342	2134	REV	KREV	16

[a]Balloon sites were used to access soundings, while surface meteorology sites were used to access surface observations.

"maybe" cases typically had weak elevated temperature inversions where a clear stable layer was not present or had higher surface wind speeds than the clear CAP cases. PCAP events were based on at least two CAP days in a row, or three radiosondes characterized "yes" or "maybe" CAPs. See Table 2, below, for the number of PCAP days determined with this method at each site in January 2016.

Radiosonde data were also used to find the observed PBL height at the Boise, Denver, Hawthorne, and Reno sites to evaluate modeled PBL heights. Given the wintertime conditions, we chose to use the bulk Richardson number approach to determine PBL heights using sounding data and the corresponding WRF output files on a twice-daily basis (0:00 and 12:00 UTC soundings).[66,69] Daily observations of surface relative humidity, temperature, wind speed and direction at the BOI, DNR, REV, and SLC airports were accessed from the MesoWest API to evaluate the WRF model performance for Boise, Denver, Reno, and Salt Lake City (Bountiful and Hawthorne), respectively.

We took observed total and speciated $PM_{2.5}$ concentrations from each CSN station over January 2016 and used one-half of the species MDL to fill in missing or negative values.[70] For observed ionic (NO_3^-, NH_4^+, SO_4^{2-}) and carbonaceous (organic carbon and elemental carbon) $PM_{2.5}$, we used a correction method with collocated IMPROVE monitors to compensate for the network changing its method at that time.[71] We calculated model performance metrics[72−74] for speciated $PM_{2.5}$ using this corrected CSN data. These metrics are available in Supporting Information, Tables S-2 (metric definitions and ranges), S-3 (total $PM_{2.5}$ performance) and S-5 though S-7 (chemically speciated $PM_{2.5}$ performance).

3. RESULTS AND DISCUSSION

3.1. Chemical Mechanism Impacts on Annual Statistics and Total $PM_{2.5}$ Performance. The public health-focused NAAQS, promulgated in February of 2024, is 9 $\mu g\ m^{-3}$ for annual mean $PM_{2.5}$ concentrations (on a rolling 3-year basis).[17] We utilize a one-month simulation period and compare model outputs to the annual standard to assess the possible impact of the new rule. Using observations for February-December 2016 and the simulations of January 2016, annual means at the five study sites were below 12 $\mu g\ m^{-3}$ (the 2012 primary, annual standard) and the new 2024 standard, with annual means ranging from 2.74 to 8.27 $\mu g\ m^{-3}$. However, the number of days exceeding 35 $\mu g\ m^{-3}$ ranged from 0 to 10 (see S.I. Table S-4). Using January 2016 observations from the same source, we evaluate the model performance for total $PM_{2.5}$ using standard performance metrics.[72−75]

Total $PM_{2.5}$ performance statistics are shown in Figure 2. Models A and B simulated higher concentrations than models C and D which sometimes resulted in positive biases, though all the models agreed in directionality and order of magnitude

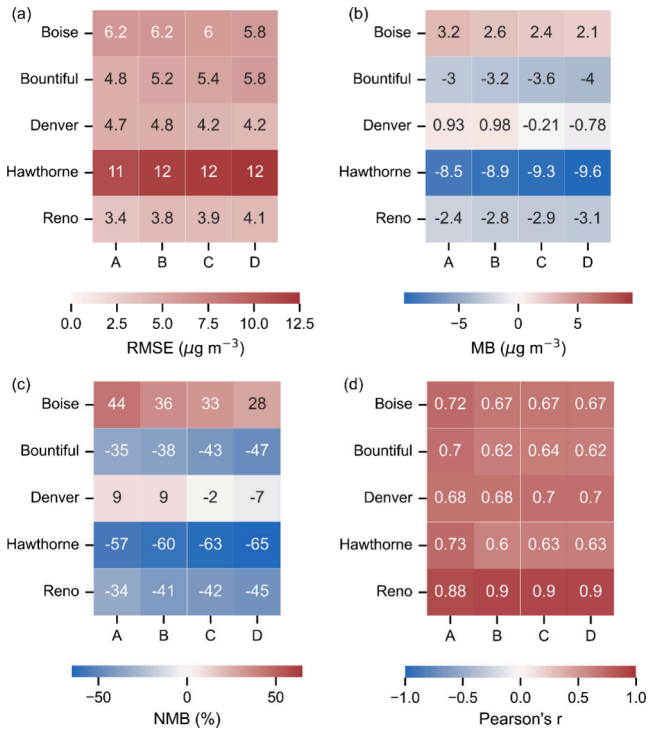

Figure 2. Heatmaps of simulated total $PM_{2.5}$ (a) root-mean-square error, (b) mean bias (MB), (c) normalized mean bias (NMB), and (d) root-mean-square error (RMSE), compared to daily averaged Federal Reference Method and Federal Equivalent Method observations. N = 31 days for all sites, the total simulation period.

of performance statistics. Using ranges of performance statistics from literature,[72] we found that models met or exceeded literature IQR (r > 0.4) for Pearson's r in all cases, but only met or exceeded 4 (8) cases for NMB (MB).[72,75] Denver met or exceeded performance goals more than other study sites, being the only site with NMB within literature values (IQR of −21.1 to 10.4% and goal of < ± 10%) and one of 2 sites with MB within literature IQR (−0.9 to 1.8 $\mu g\ m^{-3}$). All models met or outperformed literature RMSE (IQR of 5.9 to 10.4 $\mu g\ m^{-3}$) at the same sites but did not show significant differences within the same site.[72]

When comparing models B through D to the default A on an hourly basis (the finest temporal resolution in the model outputs), we can get a larger sample for comparison of the mechanisms. Using a one-way analysis of variance test (ANOVA) on hourly modeled $PM_{2.5}$ at all sites, we found that these differences were likely to be the result of the choice of mechanism ($F = 6.37$, $p \ll 0.05$) rather than stochastic variability within the model. We see a similar, stronger result from ANOVA in secondary $PM_{2.5}$ ($F = 107$, $p \ll 0.05$). Primary $PM_{2.5}$ ($F = 2.6$, $p \ll 0.05$) gave a much lower result which indicates that more of the intermodel differences can be

https://doi.org/10.1021/acsestair.4c00139
ACS EST Air 2025, 2, 162−174

ascribed to other processes in the model. Mann−Whitney U tests on models B-D versus model A showed that the distributions of total and secondary PM differed significantly: U ranged from 51.1 to 56.8% of the maximum value, $n_1 = n_2 = 5952$, $p < 0.05$, two-tailed.

3.2. Total $PM_{2.5}$ Performance during PCAP Episodes. The five sites with PCAP episodes during the study period can also be used to see how model performance changes during PCAPs and the relative behavior of the four models. Figure 3, below, compares the NMB performance between PCAP and non-PCAP days.

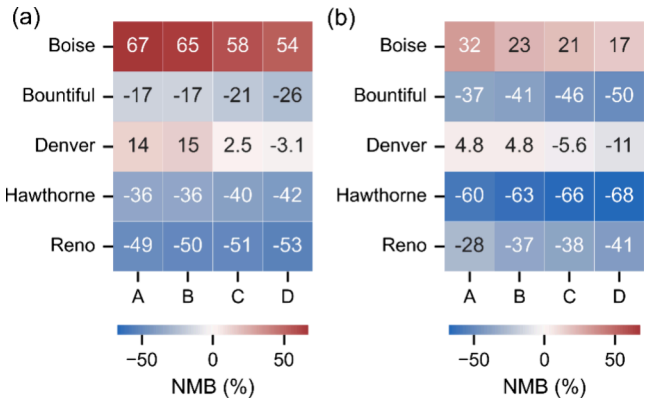

Figure 3. Heatmaps of normalized mean biases (NMB) for modeled total $PM_{2.5}$ during (a) non-PCAP and (b) PCAP days, computed using 24-h average FRM observations. Full tabulated results are available in the Supporting Information, Table S-3. The number of PCAP days were as follows: 17 in Boise, 23 in Bountiful and Hawthorne, 15 in Denver, and 16 in Reno.

There is no uniform change in site performance between the PCAP episodes and non-PCAPs. Performance in Hawthorne and Bountiful improved for all metrics during non-PCAP episodes, but Boise NMB markedly improved during PCAPs along with slight improvements in MB and RMSE in the same periods (see Table S-3 for these metrics). In Denver, models C and D had negative NMB and MB during PCAPs while A and B had positive biases, though it should be noted that MB for all models was between −2 and 2 $\mu g\ m^{-3}$. Finally, models in Reno had negative biases for both PCAPs and non-PCAPs, but RMSE improved during non-PCAPs while NMB and MB worsened.

We can see that (except in Boise and Denver) all models underestimated $PM_{2.5}$ concentrations during PCAP episodes across sites. Modeled concentrations also diverged during PCAPs, with A simulating higher concentrations than models B-D, but still lower than observed $PM_{2.5}$. During non-PCAP days, however, the models agreed more. In low-biased sites like Bountiful, while non-PCAP simulations were still lower than observations, model performance markedly improved and converged versus PCAP days (NMB ranging from −50 to −39% during PCAPs and −26 to −17% during non-PCAPs).

The better performance during non-PCAPs at Bountiful, Hawthorne, and Reno suggests that bulk transport (advection and diffusion) of pollution may be captured better by WRF and CMAQ in the absence of PCAP conditions. Similarly, simulated $PM_{2.5}$ concentrations at Boise and Denver during non-PCAPs agree with observations better than during PCAPs. However, since Boise and Denver have high, positive biases during PCAPs, it is likely that this performance difference

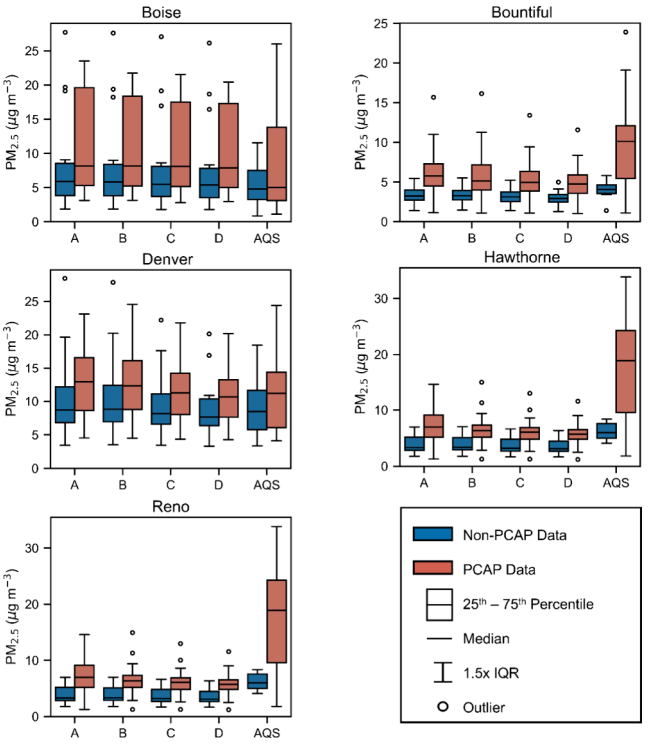

Figure 4. Box and whisker plots of simulated and observed ("AQS" on the *x*-axis) total $PM_{2.5}$ concentrations at all sites on a 24-h basis, separated by non-PCAP and PCAP days.

between sites is due to a combination of emissions and meteorology. Recent studies in the Salt Lake Valley have found that halogen emissions (chlorine and bromine) from a magnesium plant on the shore of the Great Salt Lake contributed to a significant ozone depletion in the wintertime.[76] Bromine emissions are not required to be reported for the National Emissions Inventory,[76] and similar situations of underreported emissions may contribute to the poor performance in Reno and the Salt Lake Valley sites.

3.3. Evaluating Model Meteorology. Figure 5, below, compares modeled and observed values of two meteorological parameters in the WRF model: PBL height and relative humidity (RH). Similar scatter plot comparisons for 10-m wind speed and surface temperature can be found in the Supporting Information, Figure S-1. Modeled RH at the surface corresponds well with observations on a 8-h or longer basis, but hourly observations show larger dips in RH at night than simulated in the model, leading to a positive bias at every site. Further, simulated RH is higher on average than observations during PCAPs. This behavior is seen at all four sites, but is most apparent in Denver and Reno.

This could have significant implications for model performance, as aerosol chemistry and formation are modulated by relative humidity.[77,78] Since RH is biased high at these times, it could lead to higher simulated mass concentrations of aerosol salts that either experience a hysteresis effect with RH or grow hygroscopically.[79] However, we have seen already that all four models often undersimulated total $PM_{2.5}$ concentrations, with some exceptions in Denver and Boise. From this, we can either assume that this mechanism of aerosol growth is not significant during these study conditions (unlikely), or that the undersimulation of total $PM_{2.5}$ concentrations might be due to other meteorological parameters, such as PBL height, or an

https://doi.org/10.1021/acsestair.4c00139
ACS EST Air 2025, 2, 162−174

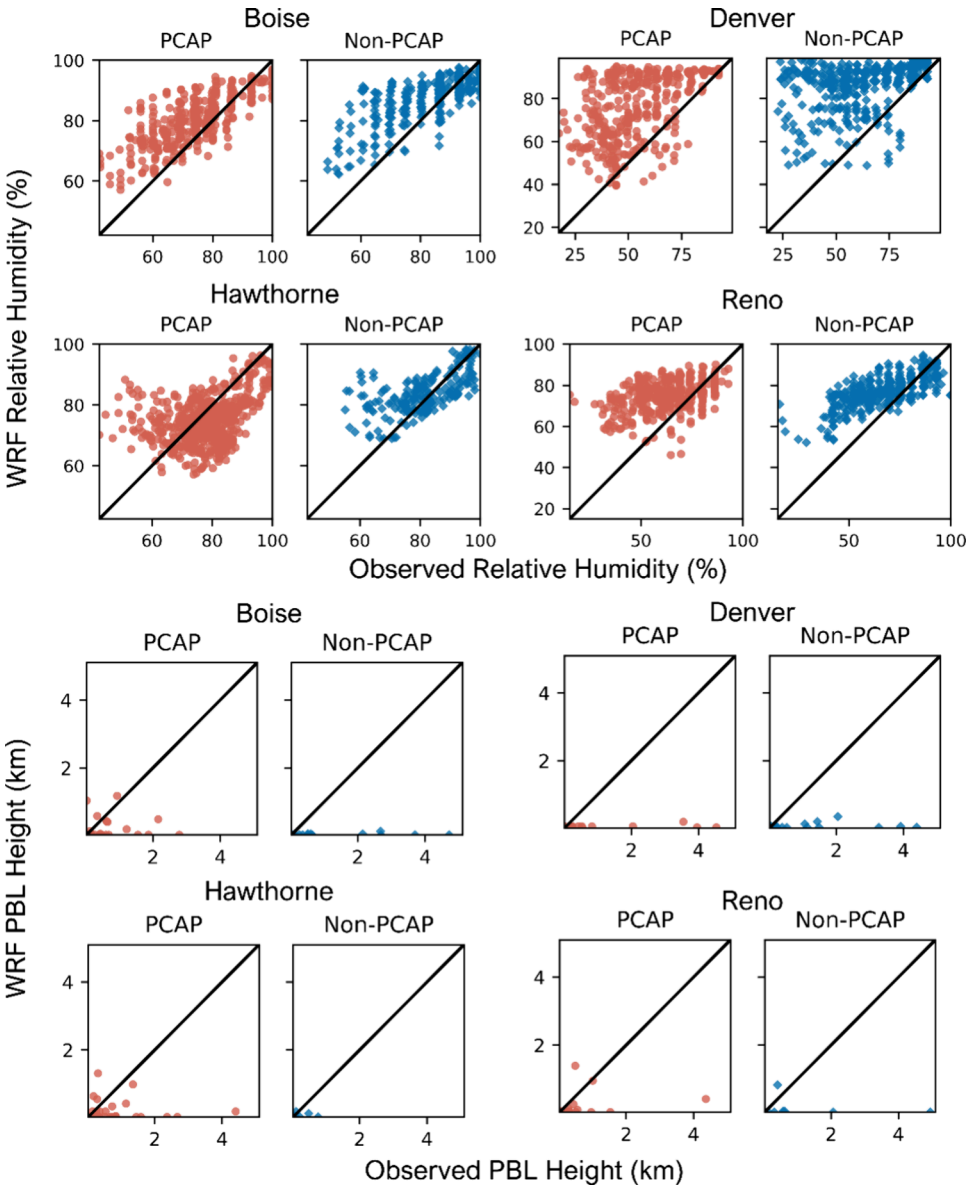

Figure 5. Scatter plot comparisons of observations versus WRF outputs of relative humidity (top) and PBL height below 5 km (bottom). Left panels at each site show performance during PCAPs, right panels for non-PCAPs.

underestimation of emissions, which would explain the relative consistency between models here.

Model performance for PBL height versus observations is more difficult to evaluate. First, the performance is not consistent across the four sites, nor is it uniform for PCAPs versus non-CAPs. Both simulated and observed PBL heights were higher than expected in these wintertime conditions, and oversimulated heights versus observations were only observed in mixed layer heights below 1 km. PBL height biases versus observations could be due to the model vertical resolution versus sondes—there being 35 total layers in the model and 14 under 1 km above the surface, and often multiple sonde data points were in the same model layer. This may also be a consequence of the coarse horizontal grid, which would especially impact the surface turbulence and boundary layer parts of WRF.[23] Performance statistics show this poor performance across the sites: NMB for PBLH below 5 km was −92% at Boise, −97% at Denver, −83% at Hawthorne, and −85% at Reno. Smaller biases for all PBLH values (see Table S-6) at Boise and Denver could be part of the reason for the occasional oversimulation of $PM_{2.5}$ discussed earlier, but Boise still has a positive bias for PBL height. This suggests that there are other factors at play, possibly a positive bias in surface temperature and modeled wind speeds in Boise that is not seen in Denver (see Figure S-1). Performance statistics for these parameters are available in the Supporting Information, Tables S-5 and S-6.

These discrepancies in modeled meteorology versus observations are to be expected, as the model horizontal grid is too coarse to resolve flows around the mountainous topography in these sites. However, even a 4 km grid, which is the finest scale possible when using emissions inputs provided for CMAQ simulations, cannot capture these dynamics in areas like the Wasatch Front in Utah.[48] The oversimulation of PBL height can contribute to a dilution of pollution within the mixed layer and an oversimulation of horizontal advection of pollution out of model grid cells, thereby causing lower simulated concentrations of $PM_{2.5}$. This

https://doi.org/10.1021/acsestair.4c00139
ACS EST Air 2025, 2, 162−174

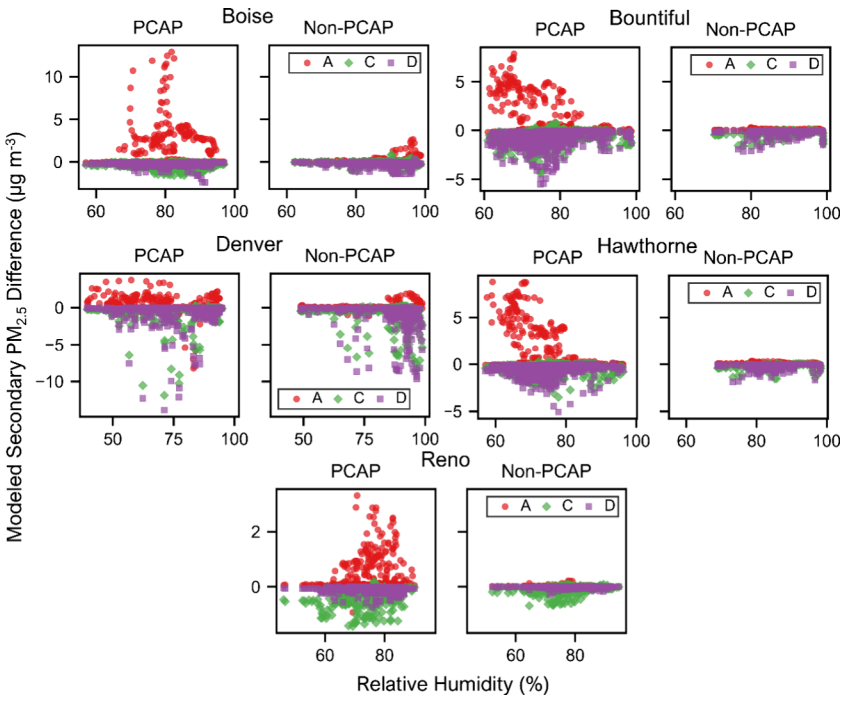

Figure 6. Scatter plots of hourly A, C, and D modeled secondary $PM_{2.5}$ (minus model B) versus relative humidity at all sites, separated by PCAPs and non-PCAP panels.

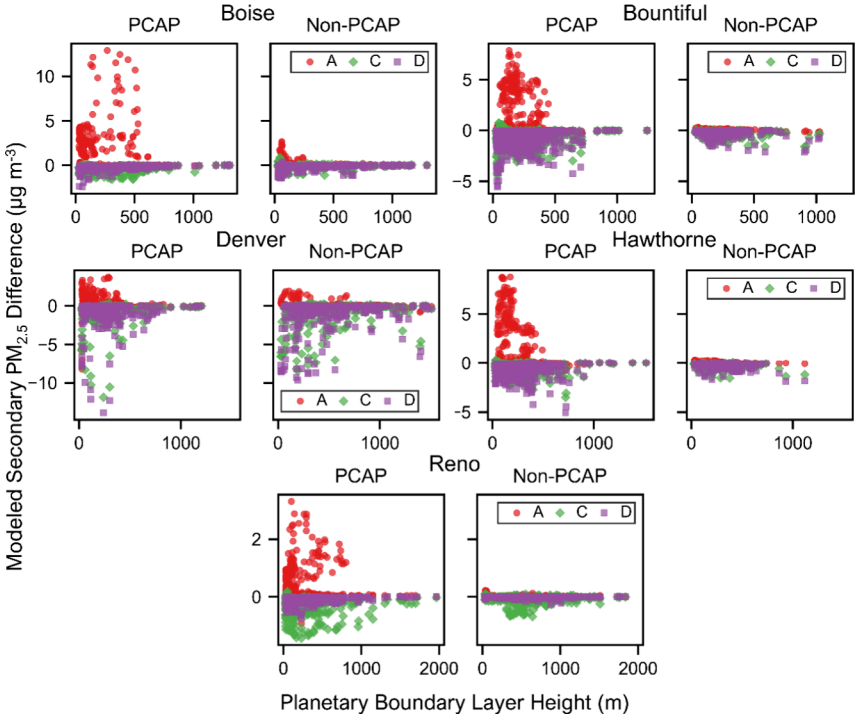

Figure 7. Scatter plots of hourly A, C, and D modeled secondary $PM_{2.5}$ (minus model B) versus PBL height at all sites, separated by PCAPs and non-PCAP panels.

should be taken into account when examining model performance versus observed concentrations. However, as this meteorology is consistent across models, we can still examine the behavior of these models as it varies with meteorology.

3.4. Intermechanism Differences in Secondary $PM_{2.5}$ Across Meteorological Variables. Meteorological conditions can impact particulate matter concentrations in varying ways, e.g., increased humidity allows more secondary PM to condense and accumulate, especially nitrates.[15,16,80] In Figures 6 (relative humidity) and 7 (PBL height), below, we see that model B-D simulations of secondary $PM_{2.5}$ at Reno are much lower than model A during PCAPs, with largest biases around a relative humidity of 80% and a PBL height less than 500 m. Conversely, during non-PCAP periods we see very low intermechanism differences, but the largest of these small

https://doi.org/10.1021/acsestair.4c00139
ACS EST Air 2025, 2, 162−174

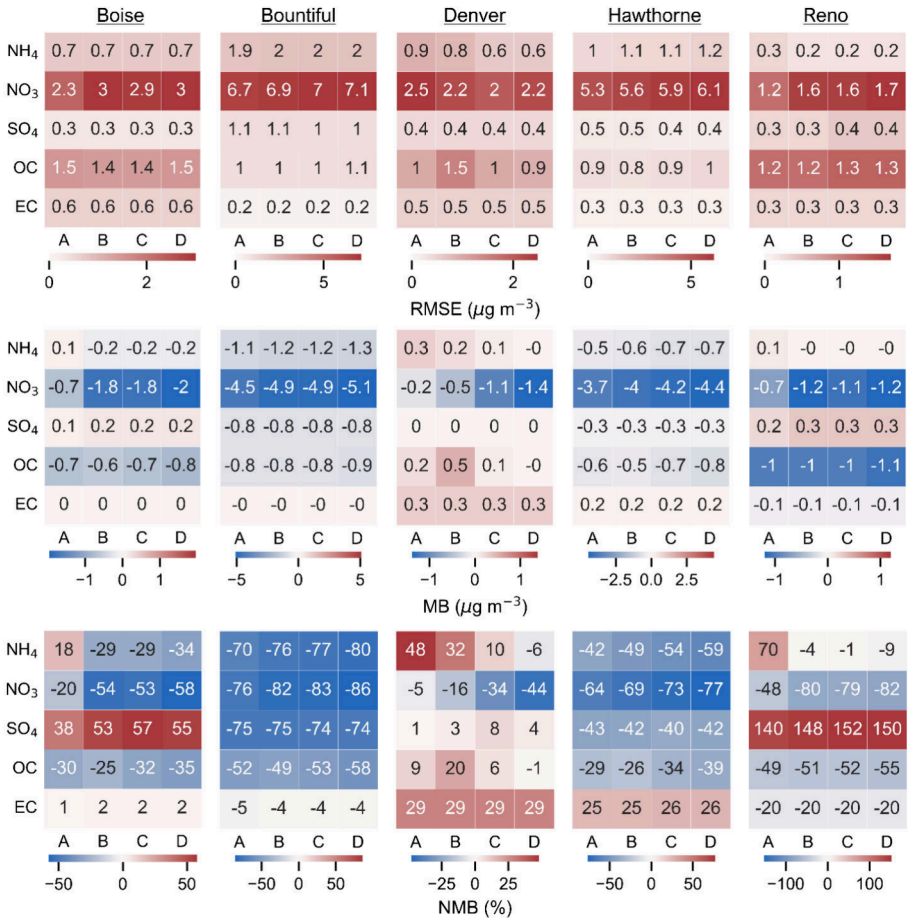

Figure 8. Heatmaps of performance metrics (RMSE, MB, NMB) calculated from CSN speciated $PM_{2.5}$ observations for all available days in January, both PCAPs and non-PCAPs. N = 11 for Reno; N = 8 for Boise, Denver, and Hawthorne; N = 6 for Bountiful. Tabulated statistics, including metals and chlorine performance, are included in the S.I. in Tables S-5 through S-7.

biases are in the same range of relative humidity and PBL height as during PCAPs. This is likely due to WRF simulating relative humidity and PBL height, among other variables, more accurately during non-PCAP episodes.

Intermechanism differencees of total and secondary $PM_{2.5}$ show similar behavior, while primary $PM_{2.5}$ does not significantly change with mechanism choice or meteorology. It is apparent that the differences in total $PM_{2.5}$ come from how each mechanism handles secondary $PM_{2.5}$. Intermechanism differencees during non-PCAPs for secondary $PM_{2.5}$ are higher than total $PM_{2.5}$, which speaks to mechanism differences that produce different estimates of secondary $PM_{2.5}$. However, the PCAP/non-PCAP differences between intermechanism differences for total or secondary $PM_{2.5}$ are much higher than the difference between total and secondary PM biases. This indicates that the "baseline" differences in model behavior from either treatment of gas-phase organics and nitrogen by the chemical mechanisms or of hygroscopic aerosol growth by the aerosol modules are amplified during PCAPs, likely also due to biases in the simulated meteorology during these episodes. This amplification of intermechanism differences repeats at all other PCAP sites except for Denver. There, non-PCAP model differences are larger than those during PCAPs, and model B versus model A is much smaller than the C-A and D−A differences. This difference between the intermechanism differences could be due to the relative importance of gas-phase chemistry differences over aerosol parametrizations in Denver.

Reno and Boise have intermechanism difference peaks at 80% relative humidity. This behavior may be connected to ammonium nitrate, as this salt has observed increases in concentrations during PCAPs and 80% relative humidity is its known deliquescence point in PCAP conditions.[15,79] However, other sites have intermechanism difference peaks at relative humidity less than 70% (Salt Lake Valley, Bountiful and Hawthorne) and over 90% (Denver), which could be connected to the deliquescence points of other salts of inorganic ions.[79,81] This is not the only source of the intermechanism variability, however, as we still see amplified differences over the whole RH and PBLH domains during PCAPs. However, nitrate, ammonium, and organic carbon have the highest differences between models A and B in the relative humidity range of 75−85%, with nitrate accounting for most of the differences in secondary $PM_{2.5}$ for every site except Denver. Ammonium also varied between mechanisms in this RH range, but not to the same magnitude as nitrate or organic carbon, which was the highest contributor to intermechanism differences in Denver. These differences were also much higher during PCAPs.

3.5. Chemically Speciated $PM_{2.5}$ Performance. While U.S. standards govern total $PM_{2.5}$, examining the composition of modeled concentrations can be a valuable tool for assessing the performance of chemical mechanisms under the conditions

https://doi.org/10.1021/acsestair.4c00139
ACS EST Air 2025, 2, 162−174

of interest. Chemical speciation information can provide insight into the source-specific contributions to model biases.[82] It is also important for estimating health impacts of ambient pollution, as the composition of particulate matter can affect the response to exposure.[83,84] Figure 8, below, shows the results of three performance metrics for all models and sites using corrected CSN observations of ammonium, nitrate, sulfate, organic carbon (OC), and elemental carbon (EC) $PM_{2.5}$.

In contrast with daily total $PM_{2.5}$, discussed above in sections 3.1 and 3.2, performance for speciated $PM_{2.5}$ (see Figure 8) often did not fall within the literature IQRs. Of the five species of PM for which Simon et al. (2012)[72] compiled performance statistics (sulfate, nitrate, ammonium, elemental carbon, and organic carbon), elemental carbon met performance goals the most (all model/site NMB within Emery et al. criterion of ±40% and Simon et al. RMSE IQR of 0.3 to 0.8 $\mu g\ m^{-3}$).[72,75] Model B-D ammonium met NMB IQR (−16.8 to 6.5%) only once, and A did not fall in NMB or MB IQRs (MB between −0.2 and 0.0 $\mu g\ m^{-3}$) at all.[72] Organic carbon also exhibited variable performance between models: A and B fell within NMB (−30.8 to 19.6%) and MB (−0.8 to 0.0 $\mu g\ m^{-3}$) IQRs more than C and D, but all models fell within or beat literature RMSE IQR (2.0 to 3.4 $\mu g\ m^{-3}$).[72]

At all sites and for most species of $PM_{2.5}$, we see relatively similar performance across models for RMSE, while NMB and MB have more variability, especially between model A and B-D. Ammonium and nitrate showed the greatest intermodel variability in performance. In contrast, elemental carbon and metals like sodium had similar performance across all models (see Supporting Information, Tables S-5 through S-7 for tabulated results including metals). For species we designated as "secondary," such as nitrate and ammonium, models A and B-D often performed differently, as in Denver where nitrate NMB for A was −5% while models B-D had NMB ranging from −16% to −44%. As A was the only simulation to use the AERO7 module, this divergence in performance between it and the other models is not an unexpected result. This is not a uniform pattern across the secondary species (sulfate, nitrate, ammonium, organic carbon, and chloride), but the smaller differences between model performance metrics for sulfate and organic carbon may be impacted by lower observed and simulated concentrations of these species. The very high NMBs for chloride at all sites (Table S-5) is due to the magnitude of the observed concentrations, less than 0.1 $\mu g\ m^{-3}$ on average, and like sulfate and organic carbon remains relatively consistent between models.

Also of note is the performance at Reno, where model A had a different NMB for ammonium (70%) than models B-D (−9.3% to −0.87%) (see Table S-6). This is an unexpected result as the CMAQ aerosol module, the unifying difference between model A and B-D, does not explicitly deal with ammonium. We can see similar behavior in ammonium performance at Denver, as well, but with a smaller difference between A and B than between A and C or D. This would indicate that the gas and aerosol chemistry are both drivers of these differences in ammonium performance. This discrepancy could be a result of thermodynamics modeled with ISORROPIA-II in the CMAQ aerosol module, which takes total concentrations of ammonia, nitrate, and chlorine species as inputs and then finds the partitioning between and concentrations of both gas and aerosol phases.[34,63] Previous studies have found that ammonium concentrations in both CMAQ and ISORROPIA are sensitive to pH and gaseous precursor emissions.[64] This discrepancy between models, then, may be caused by differences in concentrations of gaseous precursors that then propagate through the aerosol module.

4. IMPLICATIONS AND UNCERTAINTIES

Previous studies have shown that implemented science options in CMAQ and the WRF simulations used as inputs can significantly impact the CMAQ results.[28,39,40] In this study, we sought to examine the interaction between these parameters in the western United States for wintertime, where frequent PCAP episodes are linked to elevated concentrations of air pollution[9,14,15] and increased adverse health outcomes.[10] We compared four of the most common chemical mechanisms in one-month CMAQ simulations and examined 2016 observed $PM_{2.5}$ in the relation to the new annual NAAQS. The differences between the four mechanisms in CMAQ are concerning for longer-term simulations of western U.S. air quality in the wintertime, especially during PCAP episodes.

We quantified model performance for total and chemically speciated $PM_{2.5}$ and compared performance during PCAPs. Comparisons of modeled and observed $PM_{2.5}$ over the study period (Figure 4) show that even the highest simulated concentrations of PM during PCAP episodes are usually lower than the observed concentrations by at least 1 $\mu g\ m^{-3}$, and often the difference between observation and model is much larger than that during non-PCAPs. Given the importance of meteorological inputs to CMAQ, we also compared model meteorology to observations at collocated sites and then examined how intermechanism differences of secondary $PM_{2.5}$ changed with model meteorology and across PCAP conditions. The bulk of the differences in simulated total $PM_{2.5}$ concentrations can be attributed to differences in secondary PM, which are due to the choice of chemical mechanism and are amplified at certain values of simulated PBLH and RH. Of particular concern in these secondary aerosols are nitrate, ammonium, and organic carbon, species that dominate $PM_{2.5}$ composition during PCAPs. They also have strong, nonlinear relationships with humidity and require more direct observations for full understanding of their chemical and physical dynamics.[15,23,80,85]

CMAQ and other chemical transport models are used for future attainment demonstrations and proof of proposed emission controls in State Implementation Plans for areas designated as nonattainment.[18,19] Choosing the chemical mechanism that best reproduces wintertime total particulate matter concentrations is essential for these demonstrations.[86] Since these models are run to demonstrate the efficacy of emission controls, it follows that source apportionment methods for total and speciated $PM_{2.5}$ will need models that capture wintertime chemistry particularly accurately in the absence of input or parameter tuning. It should be noted that the simulations examined in this work are distinct from demonstration models, and as they stand would not be acceptable for that purpose given the coarse horizontal grid and poor performance.

This analysis has demonstrated the notable difference between the mechanisms in both total and speciated $PM_{2.5}$, but the mechanistic explanation for the amplification of the intermodel differences during PCAPs has not been confirmed. Examining internal model process rates (e.g., vertical advection, coagulation, cloud processing) and reactions involving nitrate, organic carbon, and ammonium for each

https://doi.org/10.1021/acsestair.4c00139
ACS EST Air 2025, 2, 162−174

chemistry scheme during PCAP episodes is necessary to come to a mechanistic understanding of the model divergence and possible improvements to the model.[41,42,87,88]

Since this work began, two versions of the CMAQ model (5.4 and 5.5) have been released along with the new CRACMM mechanism (available as three different options), based on the RACM2 mechanism examined here as model C.[35,89−91] Future work should implement both the new CMAQ version and the new mechanisms, which have already proven to match existing mechanism performance for ozone in the eastern U.S. summertime,[89] but not examined for the western U.S. wintertime to our knowledge.

■ ASSOCIATED CONTENT

Supporting Information

The Supporting Information is available free of charge at https://pubs.acs.org/doi/10.1021/acsestair.4c00139.

Statistical test details, summary statistics of annual observations at study sites, performance metric criteria, tabulated performance metrics for total and speciated $PM_{2.5}$, comparisons of observed and simulated surface temperature and 10 m wind speed at all sites, and tabulated data for average observed and modeled $PM_{2.5}$ during and excluding PCAPs at all sites with PCAP data (PDF)

■ AUTHOR INFORMATION

Corresponding Author

Cam M. Phelan − *Department of Civil and Environmental Engineering, University of California, Berkeley, Berkeley, California 94720, United States;* orcid.org/0000-0002-4907-1980; Email: cam_phelan@berkeley.edu

Authors

Abiola S. Lawal − *Department of Civil and Environmental Engineering, University of California, Berkeley, Berkeley, California 94720, United States; Department of Civil and Environmental Engineering, University of Connecticut, Storrs, Connecticut 06269, United States;* orcid.org/0000-0002-8542-9898

Jacob Boomsma − *Department of Chemical Engineering, University of Utah, Salt Lake City, Utah 84112, United States*

Kamaljeet Kaur − *Department of Chemical Engineering, University of Utah, Salt Lake City, Utah 84112, United States*

Kerry E. Kelly − *Department of Chemical Engineering, University of Utah, Salt Lake City, Utah 84112, United States;* orcid.org/0000-0002-2232-3092

Heather A. Holmes − *Department of Chemical Engineering, University of Utah, Salt Lake City, Utah 84112, United States;* orcid.org/0000-0002-0827-7456

Cesunica E. Ivey − *Department of Civil and Environmental Engineering, University of California, Berkeley, Berkeley, California 94720, United States;* orcid.org/0000-0002-4740-2627

Complete contact information is available at: https://pubs.acs.org/10.1021/acsestair.4c00139

Notes

The content is solely the responsibility of the authors and does not necessarily represent the official views of the National Institutes of Health.

The authors declare no competing financial interest.

■ ACKNOWLEDGMENTS

Research reported in this manuscript was in part supported by the National Institute of Environmental Health Sciences of the National Institutes of Health under award number R01ES032810. This research used the Savio computational cluster resource provided by the Berkeley Research Computing program at the University of California, Berkeley (supported by the UC Berkeley Chancellor, Vice Chancellor for Research, and Chief Information Officer).

■ REFERENCES

(1) U.S. Environmental Protection Agency, Office of Air Quality Planning and Standards. *Final Regulatory Impact Analysis for the Reconsideration of the National Ambient Air Quality Standards for Particulate Matter*; EPA-452/R-24−006; Research Triangle Park, NC. 2024.

(2) Lareau, N. P.; Crosman, E.; Whiteman, C. D.; Horel, J. D.; Hoch, S. W.; Brown, W. O. J.; Horst, T. W. The Persistent Cold-Air Pool Study. *Bulletin of the American Meteorological Society* **2013**, *94* (1), 51−63.

(3) Colgan, S.; Sun, X.; Holmes, H. A. A Novel Meteorological Method to Classify Wintertime Cold-Air Pool Events. *Atmos. Environ.* **2021**, *261*, No. 118594.

(4) Lawal, A.; Phelan, C.; Do, K.; Ji, Y.; Skipper, N. T.; Shen, H.; Holmes, H.; Ivey, C. E. *Potential Impact of Future Climate on Winter Time Particulate Matter in the Western U.S.*; CMAS Center Conference. Chapel Hill, NC, 2022.

(5) Caserini, S.; Giani, P.; Cacciamani, C.; Ozgen, S.; Lonati, G. Influence of Climate Change on the Frequency of Daytime Temperature Inversions and Stagnation Events in the Po Valley: Historical Trend and Future Projections. *Atmospheric Research* **2017**, *184*, 15−23.

(6) Iacobellis, S.; Norris, J.; Kanamitsu, M.; Tyree, M.; Cayan, D. *Climate Variability and California Low-Level Temperature Inversions*. California Climate Change Center, Publication #CEC-500−2009−020-F. 2009.

(7) Horton, D. E.; Harshvardhan; Diffenbaugh, N. S. Response of Air Stagnation Frequency to Anthropogenically Enhanced Radiative Forcing. *Environ. Res. Lett.* **2012**, *7* (4), No. 044034.

(8) Bailey, A.; Chase, T. N.; Cassano, J. J.; Noone, D. Changing Temperature Inversion Characteristics in the U.S. Southwest and Relationships to Large-Scale Atmospheric Circulation. *Journal of Applied Meteorology and Climatology* **2011**, *50* (6), 1307−1323.

(9) Silcox, G. D.; Kelly, K. E.; Crosman, E. T.; Whiteman, C. D.; Allen, B. L. Wintertime PM2.5 Concentrations during Persistent, Multi-Day Cold-Air Pools in a Mountain Valley. *Atmos. Environ.* **2011**, *46*, 17−24.

(10) Beard, J. D.; Beck, C.; Graham, R.; Packham, S. C.; Traphagan, M.; Giles, R. T.; Morgan, J. G. Winter Temperature Inversions and Emergency Department Visits for Asthma in Salt Lake County, Utah, 2003−2008. *Environ. Health Perspect.* **2012**, *120* (10), 1385−1390.

(11) Deng, Q.; Deng, L.; Miao, Y.; Guo, X.; Li, Y. Particle Deposition in the Human Lung: Health Implications of Particulate Matter from Different Sources. *Environmental Research* **2019**, *169*, 237−245.

(12) Pappin, A. J.; Charman, N.; Egyed, M.; Blagden, P.; Duhamel, A.; Miville, J.; Popadic, I.; Manseau, P. M.; Marcotte, G.; Mashayekhi, R.; Racine, J.; Rittmaster, R.; Edwards, B.; Kipusi, W.; Smith-Doiron, M. Attribution of Fine Particulate Matter and Ozone Health Impacts in Canada to Domestic and US Emission Sources. *Science of The Total Environment* **2024**, *909*, 168529.

(13) Bell, M. L.; Dominici, F.; Ebisu, K.; Zeger, S. L.; Samet, J. M. Spatial and Temporal Variation in PM2.5 Chemical Composition in the United States for Health Effects Studies. *Environ. Health Perspect.* **2007**, *115* (7), 989−995.
(14) Ivey, C. E.; Balachandran, S.; Colgan, S.; Hu, Y.; Holmes, H. A. Investigating Fine Particulate Matter Sources in Salt Lake City during Persistent Cold Air Pool Events. *Atmos. Environ.* **2019**, *213*, 568−578.
(15) Baasandorj, M.; Hoch, S. W.; Bares, R.; Lin, J. C.; Brown, S. S.; Millet, D. B.; Martin, R.; Kelly, K.; Zarzana, K. J.; Whiteman, C. D.; Dube, W. P.; Tonnesen, G.; Jaramillo, I. C.; Sohl, J. Coupling between Chemical and Meteorological Processes under Persistent Cold-Air Pool Conditions: Evolution of Wintertime $PM_{2.5}$ Pollution Events and N_2O_5 Observations in Utah's Salt Lake Valley. *Environ. Sci. Technol.* **2017**, *51* (11), 5941−5950.
(16) Baasandorj, M.; Brown, S.; Hoch, S.; Crosman, E.; Long, R.; Silva, P.; Mitchell, L.; Hammond, I.; Martin, R.; Bares, R.; Lin, J.; Sohl, J.; Page, J. *2017 Utah Winter Fine Particulate Study Final Report*. 2018. https://csl.noaa.gov/groups/csl7/measurements/2017uwfps/finalreport.pdf (accessed 2024−06−01).
(17) U.S. Environmental Protection Agency. Reconsideration of the National Ambient Air Quality Standards for Particulate Matter. *Fed. Regist.* **2024**, 16202−16406.
(18) US EPA, O. *About Air Quality Implementation Plans*. https://www.epa.gov/air-quality-implementation-plans/about-air-quality-implementation-plans (accessed 2024−04−29).
(19) US EPA, O. *State Implementation Plan (SIP) Attainment Demonstration Guidance*. https://www.epa.gov/scram/state-implementation-plan-sip-attainment-demonstration-guidance (accessed 2024−04−29).
(20) Appel, K. W.; Bash, J. O.; Fahey, K. M.; Foley, K. M.; Gilliam, R. C.; Hogrefe, C.; Hutzell, W. T.; Kang, D.; Mathur, R.; Murphy, B. N.; Napelenok, S. L.; Nolte, C. G.; Pleim, J. E.; Pouliot, G. A.; Pye, H. O. T.; Ran, L.; Roselle, S. J.; Sarwar, G.; Schwede, D. B.; Sidi, F. I.; Spero, T. L.; Wong, D. C. The Community Multiscale Air Quality (CMAQ) Model Versions 5.3 and 5.3.1: System Updates and Evaluation. *Geosci Model Dev* **2021**, *14*, 2867−2897.
(21) U.S. Environmental Protection Agency. *Modeling Guidance for Demonstrating Air Quality Goals for Ozone, PM2.5, and Regional Haze*. 2018. https://www.epa.gov/sites/default/files/2020-10/documents/o3-pm-rh-modeling_guidance-2018.pdf (accessed 2024−05−30).
(22) Sun, X.; Holmes, H. A.; Xiao, H. Surface Turbulent Fluxes during Persistent Cold-Air Pool Events in the Salt Lake Valley, Utah. Part II: Simulations. *Journal of Applied Meteorology and Climatology* **2020**, *59* (6), 1029−1050.
(23) Sun, X.; Ivey, C. E.; Baker, K. R.; Nenes, A.; Lareau, N. P.; Holmes, H. A. Confronting Uncertainties of Simulated Air Pollution Concentrations during Persistent Cold Air Pool Events in the Salt Lake Valley. *Utah. Environ. Sci. Technol.* **2021**, *55* (22), 15072−15081.
(24) Reeves, H. D.; Stensrud, D. J. Synoptic-Scale Flow and Valley Cold Pool Evolution in the Western United States. *Weather and Forecasting* **2009**, *24* (6), 1625−1643.
(25) Zhong, S.; Whiteman, C. D.; Bian, X.; Shaw, W. J.; Hubbe, J. M. Meteorological Processes Affecting the Evolution of a Wintertime Cold Air Pool in the Columbia Basin. *Monthly Weather Review* **2001**, *129* (10), 2600−2613.
(26) Gillies, R. R.; Wang, S.-Y.; Booth, M. R. Atmospheric Scale Interaction on Wintertime Intermountain West Low-Level Inversions. *Weather and Forecasting* **2010**, *25* (4), 1196−1210.
(27) Holmes, H. A.; Sriramasamudram, J. K.; Pardyjak, E. R.; Whiteman, C. D. Turbulent Fluxes and Pollutant Mixing during Wintertime Air Pollution Episodes in Complex Terrain. *Environ. Sci. Technol.* **2015**, *49* (22), 13206−13214.
(28) Gilliam, R. C.; Hogrefe, C.; Godowitch, J. M.; Napelenok, S.; Mathur, R.; Rao, S. T. Impact of Inherent Meteorology Uncertainty on Air Quality Model Predictions. *JGR Atmospheres* **2015**, *120* (23), 12259−12280.
(29) Emery, C.; Jung, J.; Koo, B.; Yarwood, G. *Final Report, Improvements to CAMx Snow Cover Treatments and Carbon Bond Chemical Mechanism for Winter Ozone*; UDAQ PO 480 52000000001; Ramboll Environ: Novato, CA, 2015. https://www.camx.com/files/udaq_snowchem_final_6aug15.pdf (accessed 2024−07−30).
(30) Shareef, M.; Cho, S.; Lyder, D.; Zelensky, M.; Heckbert, S. Evaluation of Different Chemical Mechanisms on O3 and PM2.5 Predictions in Alberta, Canada. *Applied Sciences* **2022**, *12* (17), 8576.
(31) Luecken, D. J.; Yarwood, G.; Hutzell, W. T. Multipollutant Modeling of Ozone, Reactive Nitrogen and HAPs across the Continental US with CMAQ-CB6. *Atmos. Environ.* **2019**, *201*, 62−72.
(32) US EPA Office Of Research And Development. *CMAQ*, 2021. https://doi.org/10.5281/ZENODO.5213949 (accessed 2022−06−15).
(33) Pye, H. O. T.; Luecken, D. J.; Xu, L.; Boyd, C. M.; Ng, N. L.; Baker, K. R.; Ayres, B. R.; Bash, J. O.; Baumann, K.; Carter, W. P. L.; Edgerton, E.; Fry, J. L.; Hutzell, W. T.; Schwede, D. B.; Shepson, P. B. Modeling the Current and Future Roles of Particulate Organic Nitrates in the Southeastern United States. *Environ. Sci. Technol.* **2015**, *49* (24), 14195−14203.
(34) Pye, H. O. T.; Murphy, B. N.; Xu, L.; Ng, N. L.; Carlton, A. G.; Guo, H.; Weber, R.; Vasilakos, P.; Appel, K. W.; Budisulistiorini, S. H.; Surratt, J. D.; Nenes, A.; Hu, W.; Jimenez, J. L.; Isaacman-VanWertz, G.; Misztal, P. K.; Goldstein, A. H. On the Implications of Aerosol Liquid Water and Phase Separation for Organic Aerosol Mass. *Atmos Chem. Phys.* **2017**, *17* (1), 343−369.
(35) Goliff, W. S.; Stockwell, W. R.; Lawson, C. V. The Regional Atmospheric Chemistry Mechanism, Version 2. *Atmos. Environ.* **2013**, *68*, 174−185.
(36) Carter, W. P. L. Development of the SAPRC-07 Chemical Mechanism. *Atmos. Environ.* **2010**, *44* (40), 5324−5335.
(37) Carter, W. P. L. *Report to California Air Resources Board Contract 92−329 Contract 95−308*. California Air Resources Board. 2000.
(38) Carter, W. P. L. Development of a Condensed SAPRC-07 Chemical Mechanism. *Atmos. Environ.* **2010**, *44* (40), 5336−5345.
(39) Cao, L.; Li, S.; Sun, L. Study of Different Carbon Bond 6 (CB6) Mechanisms by Using a Concentration Sensitivity Analysis. *Atmospheric Chemistry and Physics* **2021**, *21* (16), 12687−12714.
(40) Stockwell, W. R.; Saunders, E.; Goliff, W. S.; Fitzgerald, R. M. A Perspective on the Development of Gas-Phase Chemical Mechanisms for Eulerian Air Quality Models. *J. Air Waste Manage. Assoc.* **2020**, *70* (1), 44−70.
(41) Byun, D.; Schere, K. L. Review of the Governing Equations, Computational Algorithms, and Other Components of the Models-3 Community Multiscale Air Quality (CMAQ) Modeling System. *Applied Mechanics Reviews* **2006**, *59* (1−6), 51−76.
(42) Byun, D. W.; Ching, J. K. S. *Science Algorithms of the EPA Models-3 Community Multiscale Air Quality (CMAQ) Modeling System*. United States Environmental Protection Agency: Research Triangle Park NC, 1999.
(43) Gery, M. W.; Whitten, G. Z.; Killus, J. P.; Dodge, M. C. A photochemical kinetics mechanism for urban and regional scale computer modeling. *J. Geophys. Res.* **1989**, *94* (D10), 12925−12956.
(44) Cai, C.; Kelly, J. T.; Avise, J. C.; Kaduwela, A. P.; Stockwell, W. R. Photochemical Modeling in California with Two Chemical Mechanisms: Model Intercomparison and Response to Emission Reductions. *J. Air Waste Manage. Assoc.* **2011**, *61* (5), 559−572.
(45) US EPA. *CMAQ Model Version 5.3 Input Data -- 1/1/2016 - 12/31/2016 12km CONUS*, 2019. https://doi.org/10.15139/S3/MHNUNE (accessed 2022−08−01).
(46) Pleim, J. E. A Combined Local and Nonlocal Closure Model for the Atmospheric Boundary Layer. Part I: Model Description and Testing. *Journal of Applied Meteorology and Climatology* **2007**, *46* (9), 1383−1395.
(47) Pleim, J. E. A Combined Local and Nonlocal Closure Model for the Atmospheric Boundary Layer. Part II: Application and Evaluation in a Mesoscale Meteorological Model. *Journal of Applied Meteorology and Climatology* **2007**, *46* (9), 1396−1409.
(48) Foster, C. S.; Crosman, E. T.; Horel, J. D. Simulations of a Cold-Air Pool in Utah's Salt Lake Valley: Sensitivity to Land Use and Snow Cover. *Boundary-Layer Meteorol* **2017**, *164* (1), 63−87.

(49) Murphy, B. N.; Woody, M. C.; Jimenez, J. L.; Carlton, A. M. G.; Hayes, P. L.; Liu, S.; Ng, N. L.; Russell, L. M.; Setyan, A.; Xu, L.; Young, J.; Zaveri, R. A.; Zhang, Q.; Pye, H. O. T. Semivolatile POA and Parameterized Total Combustion SOA in CMAQv5.2: Impacts on Source Strength and Partitioning. *Atmos. Chem. Phys.* **2017**, *17* (18), 11107−11133.
(50) Kolling, J. S.; Pleim, J. E.; Jeffries, H. E.; Vizuete, W. A Multisensor Evaluation of the Asymmetric Convective Model, Version 2, in Southeast Texas. *J. Air Waste Manag Assoc* **2013**, *63* (1), 41−53.
(51) Xiu, A.; Pleim, J. E. Development of a Land Surface Model. Part I: Application in a Mesoscale Meteorological Model. *J. Appl. Meteor. Climatol.* **2001**, *2001* (40), 192−209.
(52) Pleim, J. E. A Simple, Efficient Solution of Flux−Profile Relationships in the Atmospheric Surface Layer. *Journal of Applied Meteorology and Climatology* **2006**, *45* (2), 341−347.
(53) Thompson, G.; Field, P. R.; Rasmussen, R. M.; Hall, W. D. Explicit Forecasts of Winter Precipitation Using an Improved Bulk Microphysics Scheme. Part II: Implementation of a New Snow Parameterization. *Monthly Weather Review* **2008**, *136* (12), 5095−5115.
(54) Thompson, G.; Eidhammer, T. A Study of Aerosol Impacts on Clouds and Precipitation Development in a Large Winter Cyclone. *Journal of the Atmospheric Sciences* **2014**, *71* (10), 3636−3658.
(55) Ruiz-Arias, J. A.; Dudhia, J.; Santos-Alamillos, F. J.; Pozo-Vázquez, D. Surface Clear-sky Shortwave Radiative Closure Intercomparisons in the Weather Research and Forecasting Model. *JGR Atmospheres* **2013**, *118* (17), 9901−9913.
(56) Mlawer, E. J.; Taubman, S. J.; Brown, P. D.; Iacono, M. J.; Clough, S. A. Radiative Transfer for Inhomogeneous Atmospheres: RRTM, a Validated Correlated-k Model for the Longwave. *Journal of Geophysical Research: Atmospheres* **1997**, *102* (D14), 16663−16682.
(57) Iacono, M. J. *Final Technical Report For the Project: Application of Improved Radiation Modeling to General Circulation Models; DE-FG02−93ER61549*; 2011. https://www.osti.gov/servlets/purl/1010861 (accessed 2024−03−13).
(58) Kain, J. S. The Kain−Fritsch Convective Parameterization: An Update. *Journal of Applied Meteorology and Climatology* **2004**, *43* (1), 170−181.
(59) Wang, B.; O'Brien, R. E.; Kelly, S. T.; Shilling, J. E.; Moffet, R. C.; Gilles, M. K.; Laskin, A. Reactivity of Liquid and Semisolid Secondary Organic Carbon with Chloride and Nitrate in Atmospheric Aerosols. *J. Phys. Chem. A* **2015**, *119* (19), 4498−4508.
(60) Schuetzle, D.; Cronn, D.; Crittenden, A. L.; Charlson, R. J. Molecular Composition of Secondary Aerosol and Its Possible Origin. *Environ. Sci. Technol.* **1975**, *9* (9), 838−845.
(61) Wang, H.; Wang, X.; Yang, X.; Li, W.; Xue, L.; Wang, T.; Chen, J.; Wang, W. Mixed Chloride Aerosols and Their Atmospheric Implications: A Review. *Aerosol Air Qual. Res.* **2017**, *17* (4), 878−887.
(62) *Only Simulating Primary Particulate Matter (PPM) with CMAQ - CMAQ*. CMAS CENTER FORUM. https://forum.cmascenter.org/t/only-simulating-primary-particulate-matter-ppm-with-cmaq/3626 (accessed 2024−08−03).
(63) Fountoukis, C.; Nenes, A. ISORROPIA II: a computationally efficient thermodynamic equilibrium model for K+−Ca2+−Mg2+−NH4+−Na+−SO42−−NO3−−Cl−−H2O aerosols. *Atmos. Chem. Phys.* **2007**, *7*, 4639−4659.
(64) Lawal, A. S.; Guan, X.; Liu, C.; Henneman, L. R. F.; Vasilakos, P.; Bhogineni, V.; Weber, R. J.; Nenes, A.; Russell, A. G. Linked Response of Aerosol Acidity and Ammonia to SO2 and NOx Emissions Reductions in the United States. *Environ. Sci. Technol.* **2018**, *52* (17), 9861−9873.
(65) Jia, W.; Zhang, X.; Wang, H.; Wang, Y.; Wang, D.; Zhong, J.; Zhang, W.; Zhang, L.; Guo, L.; Lei, Y.; Wang, J.; Yang, Y.; Lin, Y. Comprehensive Evaluation of Typical Planetary Boundary Layer (PBL) Parameterization Schemes in China−Part 1: Understanding Expressiveness of Schemes for Different Regions from the Mechanism Perspective. *Geoscientific Model Development* **2023**, *16* (22), 6635−6670.
(66) Zilitinkevich, S.; Baklanov, A. Calculation Of The Height Of The Stable Boundary Layer In Practical Applications. *Boundary-Layer Meteorology* **2002**, *105* (3), 389−409.
(67) Richardson, H.; Basu, S.; Holtslag, A. A. M. Improving Stable Boundary-Layer Height Estimation Using a Stability-Dependent Critical Bulk Richardson Number. *Boundary-Layer Meteorol* **2013**, *148* (1), 93−109.
(68) University of Wyoming Atmospheric Sciences. *Wyoming Upper Air Data Repository Archive*. https://weather.uwyo.edu/upperair/bufrraob.shtml (accessed 2024−06−01).
(69) Richardson, H.; Basu, S.; Holtslag, A. A. M. Improving Stable Boundary-Layer Height Estimation Using a Stability-Dependent Critical Bulk Richardson Number. *Boundary-Layer Meteorol* **2013**, *148* (1), 93−109.
(70) Malm, W. C.; Schichtel, B. A.; Pitchford, M. L. Uncertainties in PM $_{2.5}$ Gravimetric and Speciation Measurements and What We Can Learn from Them. *J. Air Waste Manage. Assoc.* **2011**, *61* (11), 1131−1149.
(71) Kaur, K.; Krall, J. R.; Ivey, C.; Holmes, H. A.; Kelly, K. E. Impact of Chemical Speciation Network Method Changes on Time Series Ion and Carbon Species Concentrations. *Aerosol Sci. Technol.* **2024**, *58*, 1318.
(72) Simon, H.; Baker, K. R.; Phillips, S. Compilation and Interpretation of Photochemical Model Performance Statistics Published between 2006 and 2012. *Atmos. Environ.* **2012**, *61*, 124−139.
(73) Kelly, J. T.; Koplitz, S. N.; Baker, K. R.; Holder, A. L.; Pye, H. O. T.; Murphy, B. N.; Bash, J. O.; Henderson, B. H.; Possiel, N. C.; Simon, H.; Eyth, A. M.; Jang, C.; Phillips, S.; Timin, B. Assessing PM2.5 Model Performance for the Conterminous U.S. with Comparison to Model Performance Statistics from 2007−2015. *Atmos. Environ.* **2019**, *214*, No. 116872.
(74) Boylan, J. W.; Russell, A. G. PM and Light Extinction Model Performance Metrics, Goals, and Criteria for Three-Dimensional Air Quality Models. *Atmos. Environ.* **2006**, *40* (26), 4946−4959.
(75) Emery, C.; Liu, Z.; Russell, A. G.; Odman, M. T.; Yarwood, G.; Kumar, N. Recommendations on Statistics and Benchmarks to Assess Photochemical Model Performance. *J. Air Waste Manage. Assoc.* **2017**, *67* (5), 582−598.
(76) Womack, C. C.; Chace, W. S.; Wang, S.; Baasandorj, M.; Fibiger, D. L.; Franchin, A.; Goldberger, L.; Harkins, C.; Jo, D. S.; Lee, B. H.; Lin, J. C.; McDonald, B. C.; McDuffie, E. E.; Middlebrook, A. M.; Moravek, A.; Murphy, J. G.; Neuman, J. A.; Thornton, J. A.; Veres, P. R.; Brown, S. S. Midlatitude Ozone Depletion and Air Quality Impacts from Industrial Halogen Emissions in the Great Salt Lake Basin. *Environ. Sci. Technol.* **2023**, *57* (5), 1870−1881.
(77) Jia, L.; Xu, Y. Effects of Relative Humidity on Ozone and Secondary Organic Aerosol Formation from the Photooxidation of Benzene and Ethylbenzene. *Aerosol Sci. Technol.* **2014**, *48*, 1−12.
(78) Wang, H.; Ding, J.; Xu, J.; Wen, J.; Han, J.; Wang, K.; Shi, G.; Feng, Y.; Ivey, C. E.; Wang, Y.; Nenes, A.; Zhao, Q.; Russell, A. G. Aerosols in an Arid Environment: The Role of Aerosol Water Content, Particulate Acidity, Precursors, and Relative Humidity on Secondary Inorganic Aerosols. *Science of The Total Environment* **2019**, *646*, 564−572.
(79) Seinfeld, J. H.; Pandis, S. N. *Atmospheric Chemistry and Physics: From Air Pollution to Climate Change*; 2006; pp 449−452.
(80) Hallar, A. G.; Brown, S. S.; Crosman, E.; Barsanti, K. C.; Cappa, C. D.; Faloona, I.; Fast, J.; Holmes, H. A.; Horel, J.; Lin, J.; Middlebrook, A.; Mitchell, L.; Murphy, J.; Womack, C. C.; Aneja, V.; Baasandorj, M.; Bahreini, R.; Banta, R.; Bray, C.; Brewer, A.; Caulton, D.; de Gouw, J.; De Wekker, S. F. J.; Farmer, D. K.; Gaston, C. J.; Hoch, S.; Hopkins, F.; Karle, N. N.; Kelly, J. T.; Kelly, K.; Lareau, N.; Lu, K.; Mauldin, R. L.; Mallia, D. V.; Martin, R.; Mendoza, D. L.; Oldroyd, H. J.; Pichugina, Y.; Pratt, K. A.; Saide, P. E.; Silva, P. J.; Simpson, W.; Stephens, B. B.; Stutz, J.; Sullivan, A. Coupled Air Quality and Boundary-Layer Meteorology in Western U.S. Basins during Winter: Design and Rationale for a Comprehensive Study.

https://doi.org/10.1021/acsestair.4c00139
ACS EST Air 2025, 2, 162−174

Bulletin of the American Meteorological Society **2021**, *102* (10), E2012−E2033.
(81) Silvern, R. F.; Jacob, D. J.; Kim, P. S.; Marais, E. A.; Turner, J. R.; Campuzano-Jost, P.; Jimenez, J. L. Inconsistency of Ammonium−Sulfate Aerosol Ratios with Thermodynamic Models in the Eastern US: A Possible Role of Organic Aerosol. *Atmospheric Chemistry and Physics* **2017**, *17* (8), 5107−5118.
(82) Ivey, C. E.; Holmes, H. A.; Hu, Y.; Mulholland, J. A.; Russell, A. G. A Method for Quantifying Bias in Modeled Concentrations and Source Impacts for Secondary Particulate Matter. *Front. Environ. Sci. Eng.* **2016**, *10* (5), 14.
(83) Valavanidis, A.; Fiotakis, K.; Vlachogianni, T. Airborne Particulate Matter and Human Health: Toxicological Assessment and Importance of Size and Composition of Particles for Oxidative Damage and Carcinogenic Mechanisms. *J. Environ. Sci. Health C Environ. Carcinog Ecotoxicol Rev.* **2008**, *26* (4), 339−362.
(84) Pye, H. O. T.; Ward-Caviness, C. K.; Murphy, B. N.; Appel, K. W.; Seltzer, K. M. Secondary Organic Aerosol Association with Cardiorespiratory Disease Mortality in the United States. *Nat. Commun.* **2021**, *12* (1), 7215.
(85) Murphy, J. G.; Gregoire, P. K.; Tevlin, A. G.; Wentworth, G. R.; Ellis, R. A.; Markovic, M. Z.; VandenBoer, T. C. Observational Constraints on Particle Acidity Using Measurements and Modelling of Particles and Gases. *Faraday Discuss.* **2017**, *200* (0), 379−395.
(86) McClure, C. D.; Jaffe, D. A. US Particulate Matter Air Quality Improves except in Wildfire-Prone Areas. *Proc. Natl. Acad. Sci. U. S. A.* **2018**, *115* (31), 7901−7906.
(87) Carlton, A. G.; Turpin, B. J.; Altieri, K. E.; Seitzinger, S. P.; Mathur, R.; Roselle, S. J.; Weber, R. J. CMAQ Model Performance Enhanced When In-Cloud Secondary Organic Aerosol Is Included: Comparisons of Organic Carbon Predictions with Measurements. *Environ. Sci. Technol.* **2008**, *42* (23), 8798−8802.
(88) Phelan, C.; Lawal, A.; Holmes, H.; Ivey, C. Assessing CMAQ and WRF Performance for Aerosol Chemistry During Persistent Cold Air Pool (PCAP) Events; *AGU Fall Meeting Oral Presentations*, 2022.
(89) Place, B. K.; Hutzell, W. T.; Appel, K. W.; Farrell, S.; Valin, L.; Murphy, B. N.; Seltzer, K. M.; Sarwar, G.; Allen, C.; Piletic, I. R.; D'Ambro, E. L.; Saunders, E.; Simon, H.; Torres-Vasquez, A.; Pleim, J.; Schwantes, R. H.; Coggon, M. M.; Xu, L.; Stockwell, W. R.; Pye, H. O. T. Sensitivity of Northeastern US Surface Ozone Predictions to the Representation of Atmospheric Chemistry in the Community Regional Atmospheric Chemistry Multiphase Mechanism (CRACMMv1.0). *Atmos. Chem. Phys.* **2023**, *23* (16), 9173−9190.
(90) Wiser, F.; Place, B. K.; Sen, S.; Pye, H. O. T.; Yang, B.; Westervelt, D. M.; Henze, D. K.; Fiore, A. M.; McNeill, V. F. AMORE-Isoprene v1.0: A New Reduced Mechanism for Gas-Phase Isoprene Oxidation. *Geoscientific Model Development* **2023**, *16* (6), 1801−1821.
(91) Pye, H. O. T.; Place, B. K.; Murphy, B. N.; Seltzer, K. M.; D'Ambro, E. L.; Allen, C.; Piletic, I. R.; Farrell, S.; Schwantes, R. H.; Coggon, M. M.; Saunders, E.; Xu, L.; Sarwar, G.; Hutzell, W. T.; Foley, K. M.; Pouliot, G.; Bash, J.; Stockwell, W. R. Linking Gas, Particulate, and Toxic Endpoints to Air Emissions in the Community Regional Atmospheric Chemistry Multiphase Mechanism (CRACMM). *Atmospheric Chemistry and Physics* **2023**, *23* (9), 5043−5099.

https://doi.org/10.1021/acsestair.4c00139
ACS EST Air 2025, 2, 162−174